ZIBELINE INTERNATIONAL™ PUBLISHING

Earth Sciences Malaysia (ESMY)

DOI: http://doi.org/10.26480/esmy.02.2023.142.155

ISSN: 2521-5035 (Print)
ISSN: 2521-5043 (Online)
CODEN: ESMACU

RESEARCH ARTICLE

HYDROGEOCHEMICAL ANALYSIS OF WATER IN THE AYANFURI AREA: IMPLICATIONS FOR HUMAN CONSUMPTION AND IRRIGATION

Ewusi Anthony*, Samuel Edem Kodzo Tetteh, Albert Kafui Klu and Jamel Seidu

Department of Geological Engineering, Faculty of Geosciences and Environmental Studies, University of Mines and Technology, P.O. Box 237, Tarkwa, Ghana.
Corresponding Author Email: aewusi@umat.edu.gh

ARTICLE DETAILS

Article History:

Received 01 April 2023
Revised 03 May 2023
Accepted 07 June 2023
Available online 14 June 2023

ABSTRACT

The study of groundwater and surface water in the Ayanfuri area of the Central Region of Ghana has been carried out using hydrochemical analysis and geochemical modelling to determine its suitability for human consumption and irrigation purposes. A total of 77 samples were collected from community boreholes, observation boreholes, Tailing Storage Facility (TSF) boreholes, and streams and analyzed for geochemical parameters. Sodium is the dominant cation for all the sampling sites except for TSF boreholes which are calcium-dominated. Also, the dominant anion is bicarbonate for all sampling sites, except for streams that are sulphate-dominated. The hydrochemical facies in the sampling sites are Na-Mg-HCO3 (54.55%), Na-Mg-HCO3-Cl (23.08%), Na-Mg-HCO3 (22.22%), Na-Mg-HCO3-Cl (22.86%) representing community boreholes, observation boreholes, TSF borehole, and streams, respectively. Water-rock interaction, atmospheric precipitation patterns, ion exchange reactions, and breath dissolution/erosion of plagioclase feldspars serve as the mechanisms influencing the chemical composition of the various water sampling sites. The geochemical modelling reveals the signatures of calcite, dolomite, and gypsum as the main mineral phases. From the water quality guidelines of WHO and WQI classifications, the water is suitable for consumption purposes. Also, the results of the sodium adsorption ratio, sodium percentage, and magnesium hazard indicate that the water in the study area is suitable for irrigation purposes.

KEYWORDS

Factor Analysis, Saturation Index, Sodium Adsorption Ratio, Correlation Analysis, Water Quality Index

1. INTRODUCTION AND BACKGROUND

Groundwater is the preferred source of water supply for the people of Ayanfuri and its surrounding communities because surface water bodies are ephemeral and not sustainable. Globally, there have been numerous investigations on how the quality of groundwater changes with time and how to develop the resource for human consumption and agricultural activities (Hagan *et al.*, 2022). The quality of groundwater refers to the state of its chemical, physical, and biological parameters as defined by (Lasker *et al.,* 2022). That identified taste, temperature, odor, and color, among other parameters as the indicators of the physical quality of groundwater (Kumar *et al.*, 2022). However, mentioned that research should focus on the chemical and biological quality of groundwater since the resource is usually without color, odor, and taste to a large extent (Harter, 2003). The Environmental Protection Agency's drinking water programme establishes permissible amounts of inorganic and organic groundwater components, microbiological matter, and other groundwater quality parameters (Harter, 2003). For the further stated that attention must be paid to the amounts of dissolved solids that could be found in groundwater, which are usually inorganic minerals, nutrients, and trace elements. This supposition is because of the importance of groundwater resources to humanity which will become highly impaired by contamination or pollution. Groundwater contamination may be defined as an unfavourable change in groundwater quality caused by anthropogenic activities (Rathnasri and Manage, 2016).

As a alluded that many domestic, agricultural, and even industrial activities are increasingly dependent on groundwater resources (Li et al., 2022). The agreed by acknowledging that globally, irrigation and drinking water are largely constituted by groundwater (Rahaman et al., 2022). This is particularly true in arid and semi-arid climates with little or no precipitation. This motion is supported by the fact that one-third of human beings now drink water from aquifers (Balasubramanian and Saravanakumar, 2022). Despite this obvious importance, human health and plant metabolism may be detrimental by the use of water of poor quality. This a major problem in developing countries such as Ghana where the poor quality of groundwater has been linked to certain diseases such as dental and skeletal fluorosis. For instance, the World Health Organization (WHO) has identified the unavailability of clean water in developing countries as a major control of deteriorating health and life expectancies according to (Kumar and Balamurugan, 2018).

Sustainable Development Goal 6 (SDG 6) has over the years attempted to fix the poor-quality water problem by focusing on how to provide clean water for humanity all over the world (Sunkari et al., 2022). This objective thus represents a global effort to improve access to clean water. Hydrogeochemical studies have proven to be essential in delineating the hydrogeochemical evolution and suitability of groundwater for the intended purpose according to (Liu et al., 2020). For example, studies have established the high association of Total Dissolve Solids (TDS) of water with increased ions present, the Electrical Conductivity (EC) as well as salinity.

Quick Response Code	Access this article online	
	Website: www.earthsciencesmalaysia.com	**DOI:** 10.26480/esmy.02.2023.142.155

Cite The Article: Ewusi Anthony, Samuel Edem Kodzo Tetteh, Albert Kafui Klu and Jamel Seidu (2023). Hydrogeochemical Analysis of WateriIn The Ayanfuri Area: Implications for Human Consumption and Irrigation. *Earth Sciences Malaysia, 7(2): 142-155.*

In Ghana, several studies have reported the hydrochemical status of groundwater in some regions. The employed geostatistics to evaluate the contamination of groundwater and found that the resource has a good quality for drinking with reservations and suggested that geogenic processes such as ion exchange and weathering as well as anthropogenic activities including the use of fertilizers and waste disposal adversely affect groundwater quality in the Afigya Kwabre District (Agyemang, 2022). revealed that in the Garu-Tempane District, the groundwater is generally of good quality for human consumption. However, the study identified that about 10.5 % of groundwater samples showed some elevated nitrate content, implying possible human health implications (Okofo et al., 2022).

Similarly, investigated the hydrochemical status of groundwater quality in Togo and Dahomeyan aquifers in Ghana and reported that geogenic factors controlling groundwater chemistry include silicate weathering, mineral dissolution and ion exchange reactions while anthropogenic activities, adversely affecting groundwater quality include poor farming practices and sewage disposal (Sunkari et al., 2022). The study noted that owing to elevated amounts of various physical and chemical parameters with reference to WHO guideline values, groundwater in Togo and Dahomeyan aquifers in Ghana may not be suitable for human consumption (Sunkari et al., 2022). Current findings indicate that studies on the hydrogeochemical profile of groundwater warrant scientific attention.

The Ayanfuri area is noted for its historic mining activities, both legal and illegal activities. Over the past years studies on water resources have focused on surface water due to the adverse effects of illegal mining activities. The conducted research to assess the quantities of heavy metals such as Hg, Pb, As, and Zn in the Offin River in Ayanfuri, Dunkwa-on-Offin, Nkotumso and Buabenso, and the results indicated that Ayanfuri had the greatest amounts of heavy metals (Adu, 2018). As a obtained results that depicted that the radiation levels of the radionuclides: ^{238}U, ^{232}Th, and ^{40}K in rock, soils, ore samples, and gross alpha/beta analysis in water samples are within the natural levels recorded in literature and is comparable with globally acceptable values (Faanu et al., 2016). The also said that the total yearly effective dosage for public exposure is less than the 1 mSv recommended threshold by the International Commission on Radiological Protection (ICRP) (Faanu et al., 2016). In examining the quality of rainwater in the same location, (Amponsah *et al.,* 2015) discovered that rainwater may not be appropriate for drinking or other household purposes unless it is rigorously treated. Linked this poor quality to an increase in the amounts of pollutants in the atmosphere caused by anthropogenic activities such as mining (Amponsah et al., 2015). The conducted a hydrogeophysical assessment of aquifers in Ghana's Upper Denkyira East and West Districts and discovered that the Birimian rock formation is more aquifer protective than the Tarkwaian formation (Agyemang, 2021).

This study aims at rolling out a comprehensive groundwater quality assessment in the Ayanfuri area to ensure the suitability of the water for irrigation and consumption purposes. This will be done through analysis of major ions, physicochemical parameters, and trace metals. The Gibbs plots, bivariate plots, box-and-whisker plots, piper diagrams, Durov plots, statistical techniques, and GIS mapping were utilized to delineate the major water facies in the area, groundwater evolution, and controls on water chemistry.

2. Study Area

The study was conducted at Ayanfuri in the Upper Denkyira West District. The district shares boundaries in the Northwest with the Bibiani-Anhwiaso-Bekwai district, Amansie West and Amansie Central districts in the North-East, Wassa Amenfi East and Wassa Amenfi West districts in the southwest and to the South by Upper Denkyira East Municipal. Although about 3940 people live in the Ayanfuri area, the entire district has about 31300 residents.

Geologically, Ayanfuri is situated within the Kumasi basin (Figure 1). It is situated close to the basin's contact with the western flank of the Ashanti Greenstone Belt, at the extreme south-eastern portion of the West African Craton (WAC). Lithologically, most of the rocks found in the Ayanfuri area are volcaniclastics, greywackes, and argillaceous sediments, all of which belong to the Birimian metasedimentary unit. Most of these rocks have been faulted, intensely folded, and (Basin–type) granitoids are found as intrusions along certain regional structures and discontinuities.

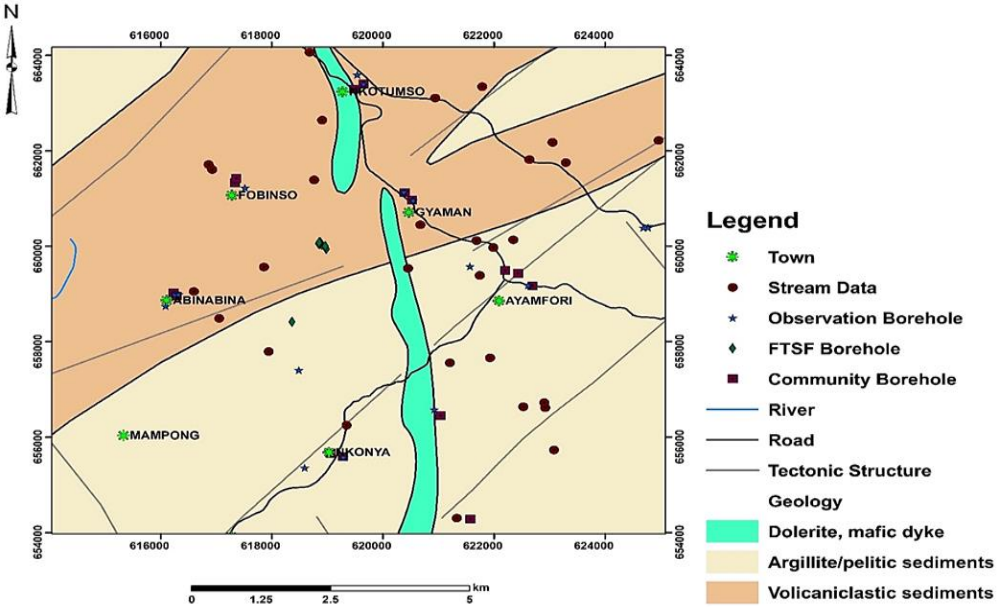

Figure 1: Geology of the Ayanfuri Area

3. Materials and Methods

3.1 Sample Acquisition

In total, 77 samples were collected in 0.5-liter polyethylene bottles. Out of these, 11 were sampled from community boreholes (Table 1), 13 were sampled from observation boreholes (Table 2), 18 from tailings storage facility (TSF) wells (Table 3), and 35 were obtained from streams (Table 4). In sampling at all locations, the sampling procedures of (Barcelona *et al.,* 1985) were strictly observed. Dilute nitric acid (10% HNO_3) was used to purify the sampling bottles after pure water was used thoroughly. This was followed by cleaning with distilled water. Prior to the collection of the samples, the wells were purged for a minimum of 5 minutes. Also, the water samples were filtered with hand-held syringes that had cellulose filter membranes and kept in ice chests at 4°C until needed for analysis.

3.2 Parameter Measurements

Physical parameters were measured with water quality probes at the point of sampling. On the other hand, chemical parameters were measured under laboratory conditions using specific meters. i.e., a flame photometer was used to measure the concentrations of Na^+ and K^+ whereas an atomic adsorption spectrometer was used to measure the concentrations of Ca^{2+} and Mg^{2+}. The concentrations of NO_3, HCO_3^-, Cl^-, SO_4^{2-}, and F^- were measured using ion chromatography. To validate the accuracy and precision of the measurements, simulated rainwater 2 (SR-2) standards were included in the measurement procedures for all ions. Details of the physical and chemical parameters of all 77 samples have been presented in Tables 1, 2, 3 and 4. These tables present the various hydrochemical parameters for samples from the community boreholes, observation wells, TSF boreholes, and stream samples respectively.

Table 1: Hydrochemical parameters for samples from community boreholes

ID	E	N	pH	Conductivity	TDS	Na	K	Mg	Ca	Cl	SO4	HCO3	NO3
PAG 1	620519	660972	5.00	131.80	65.90	18.53	0.40	2.21	1.00	14.00	20.92	14.00	12.34
PAG 2	620392	661127	6.17	227.60	113.90	20.73	0.44	5.77	7.56	10.00	6.22	112.00	1.43
PAG 3	617330	661332	5.39	109.80	55.00	15.28	0.24	2.46	1.45	12.00	1.00	24.00	0.91
PAG 6	619282	655590	5.49	226.00	113.00	9.85	0.15	4.74	1.18	10.00	4.27	44.00	0.20
PAG 7	619058	655665	6.20	286.00	143.00	16.72	0.22	8.40	4.32	6.00	23.73	100.00	0.05
PAG 10	619649	663400	5.96	116.80	58.40	22.16	0.40	8.33	3.45	10.00	22.22	90.00	0.05
PAG 11	621036	656455	5.97	110.50	55.30	11.46	0.17	4.92	1.14	6.00	5.35	58.00	0.05
PAG 13	622429	659434	6.24	311.00	156.00	24.90	0.36	9.09	7.89	14.00	18.97	108.00	2.67
PAG 14	622201	659494	6.35	310.00	155.00	24.85	0.35	8.92	7.84	12.00	18.97	112.00	2.55
PAG 16	622694	659171	6.21	320.00	161.00	25.55	0.38	9.14	7.92	16.00	20.05	120.00	2.08
PAG 8	616282	658958	6.38	240.00	121.00	29.63	0.34	8.82	3.63	10.00	1.00	146.00	0.05

Table 2: Hydrochemical parameters for samples from observation boreholes

ID	E	N	pH	Conductivity	TDS	Na	K	Mg	Ca	Cl	SO_4	HCO_3	NO_3
OPAG15	622463	622463	5.34	150.70	75.40	17.46	0.30	2.97	1.96	14.00	1.00	26.00	12.17
OPAG16	620542	660965	4.75	96.70	48.30	8.93	4.59	0.31	1.13	10.00	39.08	0.00	15.81
OPAG18	619649	663404	6.12	211.00	106.00	22.63	1.19	8.49	1.36	14.00	3.84	36.00	16.98
OPAG19	619535	663598	6.54	210.00	105.00	20.93	0.69	6.01	3.76	10.00	4.27	46.00	0.05
OPAG21	619285	655582	4.23	206.00	103.00	12.52	3.61	1.63	4.27	28.00	4.05	0.00	30.06
OPAG22	619020	655692	5.86	311.00	156.00	31.07	8.98	5.99	6.90	26.00	31.51	54.00	27.65
OPAG37	618484	657406	5.47	105.50	52.70	6.12	0.15	1.87	5.21	6.00	1.00	38.00	3.60
OPAG41	620924	656582	5.93	194.50	97.30	27.87	0.70	4.28	1.87	12.00	21.78	78.00	0.05
OPAG51	622613	659186	6.36	430.00	215.00	14.04	5.95	6.96	21.59	14.00	1.00	2.00	0.05
OPAG54	617513	661229	6.72	563.00	282.00	6.11	0.48	2.11	26.69	10.00	1.03	322.00	0.05
OPAG55	624771	660393	6.50	347.00	174.00	17.37	1.00	11.20	15.14	6.00	4.92	190.00	0.05
OPAG56	621564	659582	6.02	158.10	79.00	15.13	0.22	3.03	3.52	6.00	19.84	82.00	0.05
OPAG57	624690	660393	6.68	376.00	189.00	22.50	0.47	9.29	23.41	6.00	38.65	220.00	0.05

Table 3: Hydrochemical parameters for samples from observation boreholes

Sample ID	E	N	pH	Conductivity	TDS	Na	K	Mg	Ca	Cl	SO_4	HCO_3	NO_3
OPAG25	618185	659392	5.59	168.10	84.10	13.39	0.34	1.36	5.75	14.00	1.00	46.00	0.05
OPAG26	618442	657727	5.08	56.80	28.40	2.08	0.15	1.18	1.00	8.00	1.00	8.00	4.66
OPAG29	618904	660036	6.75	333.00	166.00	25.31	0.44	6.89	9.76	8.00	2.32	180.00	0.05
OPAG30	618873	660083	6.55	375.00	187.00	23.42	0.30	8.63	18.76	8.00	30.86	206.00	0.05
OPAG31	618861	660045	6.31	190.00	95.10	20.77	0.59	5.50	2.59	10.00	26.76	74.00	0.05
OPAG32	618846	660053	6.36	154.70	77.40	20.22	0.29	4.94	1.81	8.00	5.14	68.00	0.05
OPAG33	618853	660081	6.86	261.00	130.00	28.88	0.36	7.15	4.48	8.00	5.78	126.00	0.05
OPAG34	618981	659944	5.96	212.00	106.00	24.77	0.25	6.94	4.26	8.00	1.00	110.00	0.05
OPAG35	618887	659987	6.49	355.00	177.00	28.34	0.34	7.19	23.51	8.00	1.00	208.00	0.05
OPAG36	618964	660003	6.52	297.00	148.00	25.46	0.27	5.80	13.46	6.00	8.16	2.00	0.05
OPAG38	618364	658417	5.93	175.70	87.80	21.11	0.42	6.26	2.40	6.00	36.92	92.00	0.05
OPAG44	619474	659458	6.52	239.00	120.00	17.55	0.79	3.84	6.97	6.00	1.00	122.00	2.08
OPAG45	617838	658741	4.90	53.50	26.80	2.79	0.13	0.88	1.73	8.00	1.00	6.00	14.05
OPAG46	617773	658826	6.30	265.00	133.00	4.98	0.63	0.62	60.95	6.00	4.49	114.00	6.48
OPAG47	619674	658995	5.54	79.50	39.80	6.68	17.20	0.43	1.78	8.00	60.92	26.00	1.32
OPAG48	620697	658153	5.66	100.20	50.10	1.96	0.12	0.73	6.90	8.00	81.03	46.00	4.72
OPAG49	619225	657076	6.68	384.00	193.00	17.00	1.98	8.94	28.23	8.00	88.16	208.00	2.25
OPAG50	618447	657656	5.48	65.40	32.70	3.22	0.23	1.22	1.89	8.00	8.59	12.00	6.30

Table 4: Hydrochemical parameters for stream samples

Sample ID	E	N	pH	Conductivity	TDS	Na	K	Mg	Ca	Cl	SO_4	HCO_3	NO_3
PAS 1	621204	657559	6.2600	86.60	43.40	5.63	0.57	2.90	3.20	8.00	1.00	40.00	0.05
PAS10	620939	663111	6.1900	67.50	33.80	7.48	0.33	1.62	1.00	6.00	1.00	22.00	0.05
PAS13	616593	659055	6.7300	119.00	59.50	7.65	1.32	3.18	3.62	8.00	7.06	42.00	0.05
PAS14	623053	662181	6.5600	116.20	58.10	11.01	0.65	2.37	2.46	12.00	1.00	50.00	0.05
PAS15	622637	661819	6.7300	126.30	63.30	13.09	1.50	1.81	4.55	10.00	1.00	48.00	0.05
PAS17	617942	657795	5.8300	87.30	43.70	8.47	0.10	2.16	1.61	8.00	1.00	34.00	0.05
PAS18	622920	656619	6.2800	62.00	31.10	5.96	0.17	1.37	1.41	8.00	8.32	14.00	0.05
PAS19	622346	660137	6.6600	70.70	35.40	8.27	0.94	1.39	1.47	8.00	139.83	16.00	0.05
PAS20	621682	660121	7.6000	200.90	100.00	15.13	1.66	2.55	10.91	6.00	323.18	92.00	0.05
PAS21	620450	659540	7.2100	221.00	110.00	7.34	2.51	1.78	22.13	4.00	2.84	124.00	0.05
PAS22	623080	655733	6.3700	91.40	45.70	7.73	0.18	2.27	1.96	8.00	1.00	36.00	0.05
PAS24	620673	660453	6.0300	81.60	40.80	9.91	2.06	1.31	1.31	8.00	1.00	20.00	0.05
PAS27	618679	664069	6.8700	227.00	114.00	13.61	1.39	5.73	8.09	6.00	36.77	56.00	8.59
PAS29	618760	661393	6.7100	182.90	91.50	18.58	1.60	4.44	3.90	8.00	6.42	2.00	0.55
PAS30	616860	661717	7.1800	432.00	216.00	18.90	2.10	8.45	38.53	8.00	76.82	108.00	12.29
PAS31	618924	660808	6.6600	199.70	99.80	19.56	1.58	4.70	4.99	8.00	10.43	78.00	0.05
PAS33	616052	658481	6.2000	102.00	51.00	7.35	0.99	3.27	2.41	6.00	5.16	42.00	0.05
PAS35	621328	654304	6.1000	106.00	53.00	8.70	0.24	2.95	2.81	8.00	1.00	42.00	0.05
PAS37	622075	659559	6.9900	235.00	118.00	15.94	7.91	4.17	10.66	10.00	1.00	104.00	0.05
PAS39	617161	659441	6.7800	271.00	136.00	40.22	3.87	3.13	3.78	8.00	42.46	42.00	26.19
PAS4	618904	662646	6.4900	136.50	68.30	11.46	0.82	3.98	3.98	6.00	1.00	64.00	0.05
PAS6	621785	663348	5.9800	68.40	34.20	8.47	0.27	1.66	1.19	6.00	1.00	24.00	0.05
PAS60	621927	657664	6.4600	53.00	26.50	6.58	0.59	1.07	1.24	6.00	2.32	20.00	0.20
PAS61	617049	658490	6.9300	753.00	377.00	29.72	1.02	13.38	33.53	8.00	155.19	126.00	29.88
PAS67	621743	659392	8.5100	241.00	121.00	33.77	2.71	3.26	6.92	12.00	4.92	116.00	0.05
PAS68	622526	656638	6.8100	33.80	16.90	3.74	0.80	0.33	1.00	14.00	1.03	8.00	0.05
PAS69	619971	656497	6.1500	18.04	9.02	1.65	0.60	0.26	1.00	12.00	1.00	8.00	0.05
PAS7	621987	659975	6.5400	225.00	113.00	15.16	5.14	4.22	9.37	12.00	1.00	94.00	0.05
PAS73	617986	659196	6.3400	142.00	71.00	5.64	1.22	3.08	11.69	6.00	34.54	20.00	0.05
PAS74	617359	660058	6.3800	182.00	91.50	8.13	2.25	6.19	6.72	10.00	44.49	28.00	0.50
PAS75	617368	660098	6.4900	186.00	93.50	8.65	2.11	9.55	6.64	10.00	47.08	30.00	0.73
PAS76	(blank)	(blank)	6.8400	456.00	228.00	30.40	21.10	1.31	34.55	10.00	98.11	2.00	3.60
PAS77	(blank)	(blank)	7.3400	147.20	73.60	8.86	8.65	3.28	7.53	8.00	77.78	62.00	0.20
PAS8	624964	662222	6.5000	64.20	32.10	6.95	0.19	1.61	1.00	6.00	2.42	34.00	0.05
PAS9	623292	661755	6.5800	88.60	44.40	9.07	0.20	2.78	2.06	6.00	2.84	32.00	0.05

3.3 Data Processing and Analysis

The PHREEQC software was used to determine the mineral saturation indices whereas the water types were differentiated by Piper diagrams using the AquaChem software. Box-and-whisker plots were produced to determine the dominance of the ions within the samples. The hydrochemical factors controlling groundwater chemistry were identified using Gibbs plots with respect to evaporation of dominant crystallization, dominant precipitation, and rock dominance (Gibbs, 1970).

SPSS Statistics version 25 was used to conduct multivariate statistical analysis. The primary statistical techniques used in this research were factor analysis (FA) and principal component analysis (PCA), Pearson correlation, and hierarchical cluster analysis (HCA). These methods are used to minimise the complexity of large-scale datasets and to demonstrate the link between data components (Sunkari *et al.,* 2022). Because geochemical datasets do not have a normal distribution, they were converted before being used in multivariate analysis. The raw datasets were transformed using the centred log-ratio (CLR) transformation to make them normally distributed, consistent, and dependable (Aitchson and Greenacre, 2002). The CLR transformation is performed using the equation by Aitchison and Greenacre (2002):

Equation: $CLR(x) = \log(x_N/g(x)), \ldots\ldots\ldots, \log(x_N/g(x))$ 1

Where x is the hydrochemical parameter, g(x) is the average of the hydrochemical parameter x, and x_1 …. x_N are the concentrations of each hydrochemical parameter.

In determining the Water Quality Index (WQI) with regard to parameters such as pH, EC, TDS, Cl^-, NO_3^-, SO_4^{2-}, Na+, K+, Ca^{2+}, and Mg^{2+} in all samples, the Weighted Arithmetic Index approach was utilized. Three (3) essential steps were followed in calculating the WQI (Brown *et al.,* 1972). Weights (Wn) were first assigned to parameters that are likely to negatively impact the water quality for consumption using the following equation:

$$Wn = \frac{K}{Sn} \quad 2$$

In equation 2, $K = \frac{1}{\Sigma 1/Sn}$ and Sn represents the standard desirable value of the n^{th} parameter using WHO guideline values. Wn always corresponds to unity.

A value known as the sub-index value (Qn) was then calculated. If Vn is the mean concentration of the nth parameter, Vo is the concentration of the nth parameter in pure water, and Sn is the standard desired value, Qn is calculated using the equation below;

$$Qn = \frac{[(Vn-Vo)]}{[(Sn-Vo)]} * 100 \quad 3$$

Vo mostly has a value of 0 (zero) for all parameters except for pH where in which case Qn is calculated as QpH $= \frac{[(VpH-7)]}{[(8.5-7)]}$, where Vo for pH is represented by V_{pH}.

By dividing the product of Wn and Qn by Wn, the WQI can then be determined. This is mathematically written as follows:

$$WQI = \frac{\sum WnQn}{\sum Wn} \quad 4$$

Sodium absorbance ratio (SAR), Sodium percentage (Na%), and magnesium ratio (MR) were calculated to evaluate the suitability of the water samples for irrigation. SAR is an important parameter in evaluating whether water could be used to irrigate farmlands according to Li *et al.,* (2016) and is computed by the equation below:

$$SAR = \frac{Na^+}{(\sqrt{(Ca^{2+} + Mg^{2+})/2})} \quad 5$$

Based on the SAR values obtained, a Wilcox diagram after Wilcox (1955) was made to aid in the evaluation. Na% was utilized as a further criterion for evaluating the quality of water for irrigation using the following equation after Wilcox (1995):

$$Na\% = \frac{Na^+ + K^+}{Ca^{2+} + Mg^{2+} + Na^+ + K^+} \times 100 \quad 6$$

Water could be classified as "suitable or harmless" for irrigation if the MR values are less than 50%. Hence, the suitability of the water for irrigation was determined by the following equation:

$$MR = \frac{Mg^{2+}}{(Ca^{2+} + Mg^{2+})} \times 100 \quad 7$$

4. Results and Discussions

4.1 Geochemical Characterization and Hydrochemical Facies

The physicochemical parameters of the various samples are summarized in Table 5 and were appraised regarding standards for domestic water instituted by the World Health Organization (WHO, 2017). The pH concentrations of water from all 4 locations (community, observation, TSF boreholes, and streams) are slightly acidic and have values lower than the WHO acceptable limits of 6.5 to 8.5 (Table 1 - 5). They recorded pH varied from 5.0 to 6.38 for community boreholes, 4.23 to 6.72 for observation boreholes, and 4.9 to 6.86 for TSF boreholes, with average values of 5.68, 5.16, and 5.68 respectively. However, the stream concentrations are slightly basic which ranges from 5.83 to 8.51 with an average value of 6.64 (Table 1 - 5). The low pH levels suggest the tendency of acidic reactions within the groundwater system as an indication of the presence of volcanic rocks, while the slight alkalinity may also suggest the activity of carbonate, bicarbonate, or hydroxide compounds dissolution.

The boreholes (community, observation, TSF) and streams samples have various electrical conductivity (EC) values ranging from 109.8 to 320, 96.7 to 563, 53.5 to 384 and 18.04 to 753.0 µS/cm with average values of 217.23, 258.42, 209.61 and 168.0 µS/cm, respectively (Table 1 - 5). This suggests that the concentrations are within the acceptable limits of the World Health Organization, guideline value of 2500 µS/ cm (W.H.O, 2017). Total dissolved solids (TDS) concentrations also varied from 55 to 161, 48.3 to 282, 26.8 to 193, and 9.02 to 377.0 mg/L with average values of 108.86, 129.45, 104.57, and 84.11 mg/L respectively (Table 1 - 5), which are within the guideline value of 1000 mg/L (W.H.O, 2017). This implies that there are no notable charged species within the aquifer system.

Table 5: Summary statistics for parameters for all samples

Parameter	Range	Minimum	Maximum	Mean	Standard Deviation
Conductivity	734.9600	18.0400	753.0000	199.9317	129.9155
TDS	367.9800	9.0200	377.0000	100.0847	65.0491
HCO3	322.0000	0.0000	322.0000	69.5584	62.6961
SO4	322.1849	1.0000	323.1849	23.6730	46.5084
Na	38.5730	1.6510	40.2240	15.1820	8.8580
Cl	24.0000	4.0000	28.0000	9.2727	3.9324
Ca	59.9470	1.0000	60.9470	8.0467	10.5412
pH	4.2800	4.2300	8.5100	6.2810	0.6507
Mg	13.1230	0.2580	13.3810	4.3237	3.0450
NO3	30.0099	0.0500	30.0599	3.3161	7.1137
K	21.0010	0.1000	21.1010	1.7653	3.4310

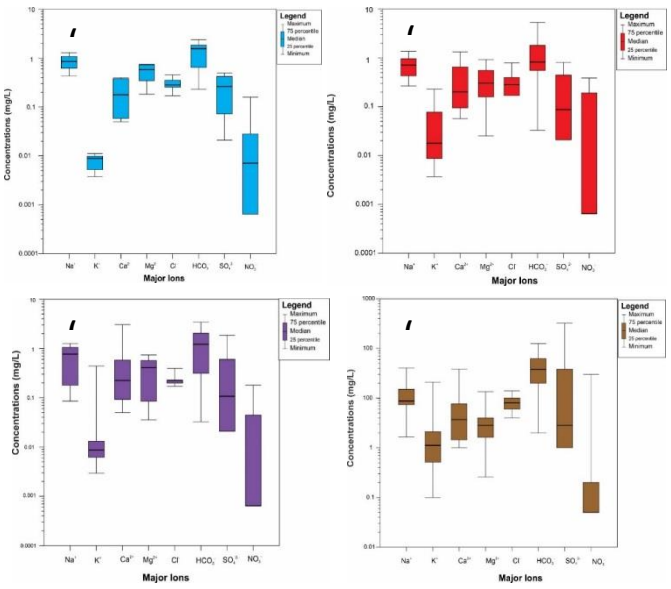

Figure 2: Box and Whisker Plots for (a) Community Boreholes, (b) Observation Wells, (c) TSF Boreholes, and (d) Stream Samples

The relative abundance of the major ions of the community boreholes occurs as $Na^+ > Mg^{2+} > Ca^{2+} > K^+$; Observation borehole occurs as $Na^+ > Ca^{2+} > Mg^{2+} > K^+$; TSF boreholes occurring as $Ca^{2+} > Na^+ > Mg^{2+} > K^+$, while the order for stream samples is $Na^+ > Ca^{2+} > K^+ > Mg^{2+}$ (Figure 2 a-d respectfully).

This implies that the predominate major cations are Na^+ and Ca^{2+}, however, none of the major cations exceeded the maximum permissible limit (200 mg/L, each) by the (WHO, 2017). The Na^+ concentrations range from 9.85 to 29.63, 6.11 to 31.07, 1.96 to 28.88, and 1.65 to 40.22 mg/L for the community, observation, TSF boreholes, and streams, with average values of 19.97, 17.13, 15.99, and 12.54 mg/L, respectively (Tables 1 - 5). This could indicate the absence of silicate weathering or salinization via ion exchange reactions (Gopinath *et al.,* 2014). The concentrations of Ca^{2+} in the study area fall within the stipulated guideline values of 200 mg/L (Tables 1, 2, 3, 4, and 5). Ca^{2+} has concentrations ranging from 1 to 7.92, 1.13 to 26.69, 1 to 60.95, and 1.0 to 38.53 for the community, observation, TSF boreholes, and streams with means values of 4.31, 8.98, 10.90, and 7.41 respectively (Table 1 - 5). The major anions occur sequentially for community, observation, and TSF boreholes as $HCO_3^- > SO_4^{2-} > Cl^- > NO_3^-$. However, the stream samples had a sequence of $SO_4^{2-} > HCO_3^- > NO_3^- > Cl^-$.

HCO_3^- has the greatest concentration among the major anions and is in the range of 14 to 146, 0 to 322, 2 to 208, and 2 to 126 mg/L for the community, observation, TSF boreholes, and stream samples with average concentrations of 84.36, 84.15, 91.89, and 48 mg/L, respectively (Table 1-5). The bicarbonate concentrations are all within the acceptable limits

stipulated by (WHO, 2017). This suggests less role of carbonic acid from precipitation and soil interactions in the water chemistry. The SO_4^{2-} concentrations vary from 1 to 23.73, 1 to 39.08, 1 to 88.16, and 1 to 323.18 mg/L of community, observation TSF boreholes, and streams with an average concentration of 12.97, 13.23, 20.29, and 32.66 mg/L, respectively (Table 1-5). This implies the role of anthropogenic activities in the research area, especially the stream locations which recorded the highest SO_4^{2-} value exceeding the limits among the other sample stations (WHO, 2017). This suggests that residents of the area may be susceptible to sulphate poisoning which could result in diarrhea and dehydration for both adults and infants. However, the concentrations of Cl^- and NO_3^-, are also within the tolerable guideline limits of (WHO, 2017). The NO_3^- concentrations may suggest an agricultural activity, sewage seepage, and other anthropogenic activities within the study area.

A Piper diagram (Figure 3) (Piper 1944) shows that the water types in the sampling sites are different from each other, with Na-Mg-HCO_3 (54.55%) as the main types of synthesis for community boreholes and other mix water-types Na-Mg-HCO_3-Cl, Na-Mg-HCO_3-SO_4, Na-SO4-Cl-HCO3 (45.45%), whereas Na-Mg-HCO_3-Cl (23.08%) was the most important chemical composition at the observation boreholes with other mix water constituents Na-HCO_3-SO_4 (15.38%), Ca-Na-Mg-HCO_3-SO_4, Mg-Na-Ca-HCO_3, Ca-HCO_3, Ca-Na-Mg-Cl, Na-Ca-HCO_3-Cl, Na-Cl-NO_3, Na-SO_4-Cl-NO_3 (7.69% each). The Predominate water type at the TSF borehole station is Na-Mg-HCO_3 (22.22%), with mix water types of about 77.78% (Na-Mg-HCO_3-SO_4, Na-Ca-HCO_3-Cl, Mg-Na-Cl-HCO_3, K-Na-SO_4-HCO_3, Ca-SO_4-HCO_3,

Na-Cl-HCO_3-SO_4, Na-Ca-Cl-NO_3-HCO_3, Na-HCO_3, Ca-HCO_3, and Na-Ca-HCO_3). Stream locations are predominantly Na-Mg-HCO_3-Cl, constituting 22.86% and the mixed water types constitute the remaining 77.14% (Na-Mg-Ca-HCO_3-Cl, Na-HCO_3-Cl, Na-Ca-HCO_3-Cl, Na-Mg-HCO_3-Cl-SO_4, Ca-HCO_3, Na-Mg-Ca-HCO_3-SO_4, Na-Mg-Ca-Cl, Ca-Na-HCO_3-SO_4, Na-Mg-HCO_3, Na-Ca-HCO_3, Na-SO_4-HCO_3, Na-HCO_3-Cl, Ca-Mg-Na-SO_4-HCO_3).

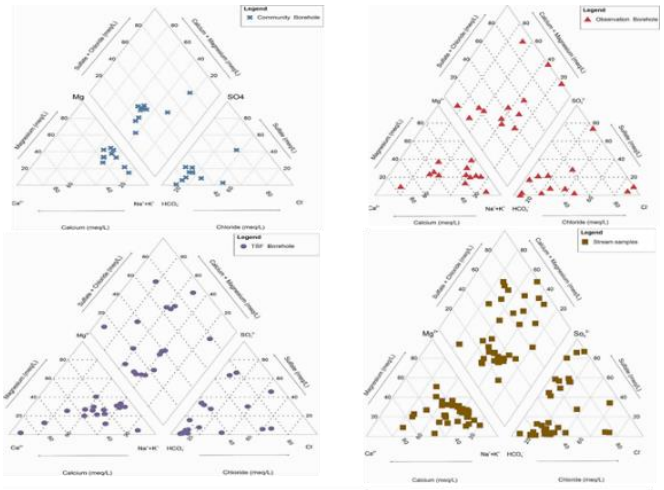

Figure 3: Piper Plots for Samples from All Four Locations

4.2 Geospatial Distribution of Hydrochemical Parameters

Four (4) maps were produced using kriging interpolation in the GIS environment to show the spatial distribution of the parameters in the study area (Figure 4) with high concentrations in red and low concentrations in blue. The "high" considered here is still within the permissible intake levels stipulated by (WHO. 2017).

The Ca distribution map (Figure 4a) generally shows low Ca concentrations across the study area. A few boreholes in the northern part, however, show isolated cases of high concentrations of Ca. The Na distribution map (Figure 4b) shows that very high Na contents are in the western portions of the study area, especially in the southwestern corner of the map, while low concentrations are within the eastern part of the area. This may indicate that the mafic dolerite dyke which runs approximately N-S in the study area (Figure 1) may be inhibiting the flow of high Na waters towards the eastern part of the area or the dyke simply prevents processes that may release more Na into the waters within the eastern part of the area.

The nitrate distribution map depicted high concentrations mainly in the southwestern part of the area whereas the sulphate distribution map depicted peak concentrations in the southern part of the area (Figure 4c). When compared to the geology (Figure 1), it is likely that areas underlain by argillite/pelitic sediments has water with high SO42- concentrations (Figure 4d) compared with those areas underlain by volcaniclastic sediments.

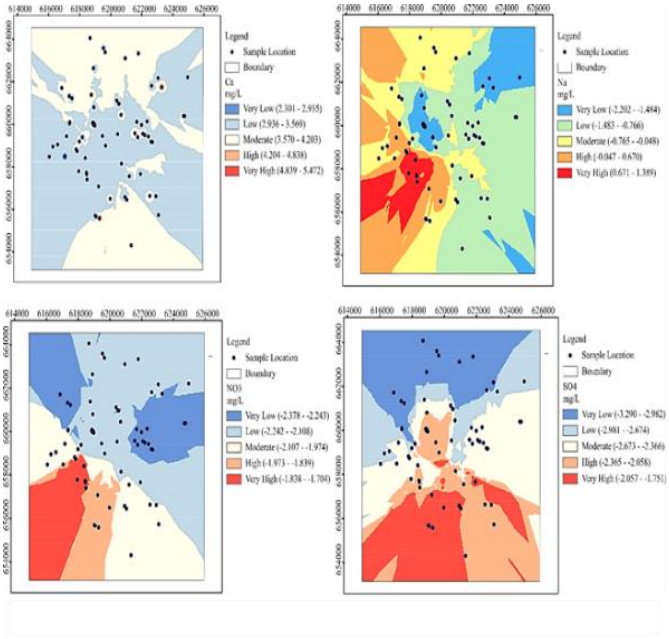

Figure 4: Geospatial Distribution of Parameters in the Study Area

4.3 Factors Controlling Groundwater Chemistry

The hydrochemical differences presented in the two regions can also be seen in the Gibbs plot (Figures 5 and 6). The connection between groundwater and aquifer characteristics is described in detail in three several aspects, including evaporation of dominant crystallization, dominant precipitation, and dominant rock (Gibbs, 1970). From the Gibbs diagram (Figures 5 and 6), all samples showed the dominant phase of the rock, except some samples within the atmospheric precipitation patterns. This is an indication of the influences of the lithology of the aquifers in groundwater and stream chemistry. Therefore, the interaction of rock with water becomes the main factor that regulates terrestrial water chemistry. However, another factor such as atmospheric precipitation also regulates the groundwater chemistry and serves as the main influencing factor from stream chemistry.

The metavolcanic sequence comprises greenstones of metamorphosed basic lava and intrusive with complementary felsic lava and pyroclastic rocks with minerals of calcite, dolomite, quartz, muscovite, orthoclase and plagioclase feldspar. Through erosion or dissolution, these minerals can serve as the major ion sources in streams and groundwater, influencing the hydrochemistry of streams and groundwater in the studied region. Na^+ shows a positive correlation with Cl^-, with some samples plotting along or close to the 1:1 line (Figure 7e, 8d, 10d), indicating breath dissolution/erosion of plagioclase feldspars and possible seawater/stream intrusion as the main sources of Na^+ and Cl^- in these groundwater samples except TSF borehole where most of the samples are plotting away from the equiline (Figure 8e). A comparison of the samples with seawater/stream indicates that seawater/stream penetrates the aquifer (Figure 10).

It can be assumed that dolomite and calcite can be dissolved, which also establishes the critical enrichment of water in Ca^{2+} and HCO_3^-. Due to the calcite dimension, the concentration of Ca^{2+}, Mg^{2+}, and HCO_3^- in the solution increases, while the dissolution of calcite increases the emission of Ca^{2+} and HCO_3^- in water. The effect of dissolving these minerals in water is based on the framework of the present study and is shown in Figures 7b, 8b, and 9b, where some samples are located along line 1:1 and below. Ca^{2+} is a common ion in the chemical structure of gypsum, dolomite, calcite, anhydride, and fluorite (Figures 7a, 8a, and 9a). According to the dissolution of anhydride, gypsum, and fluorite can also result in the dissolution of dolomite and calcite (Li et al., 2016).

The saturation indices of these minerals were estimated using PHREEQC (Parkhurst and Appelo, 1999) and are shown in Figures 11, 12, 13, and 14. The saturation indices of dolomite (0.936, 0.821, 0.642, 0.624), calcite (0.962, 0.898, 0.925, and 0.941) indicate that these samples are saturated with dolomite, calcite under current conditions and therefore reflect a longer time for community, observation, TSF boreholes, and stream samples (Ako et al., 2012). Therefore, it is clear that the predominance of

Ca^{2+} in groundwater could be associated with the gypsum dissolution, which then catalyzed the precipitation of dolomite, calcite, and anhydride in groundwater. All the groundwater samples are undersaturated with gypsum and halite (Figure 11c-d, 12c-d, 13c-d, and 14c-d). Therefore, reverse ion exchange could be the main cause of the Na^+ and Cl^- charges (Jankowski et al., 1998).

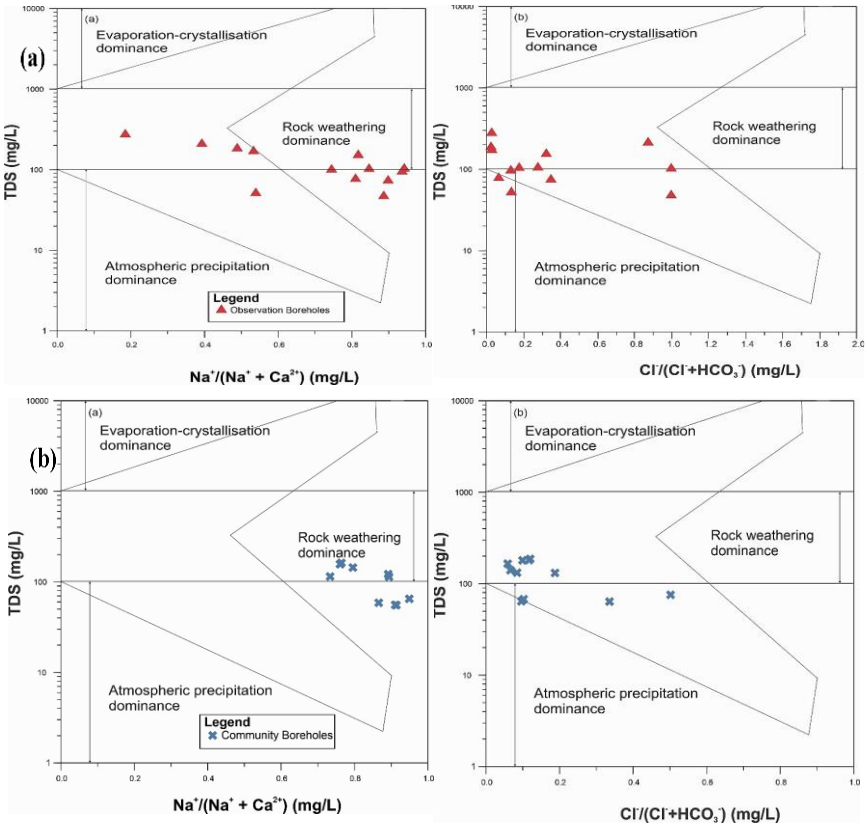

Figure 5: Gibbs Plot for (a) Observation Boreholes and (b) Community Boreholes

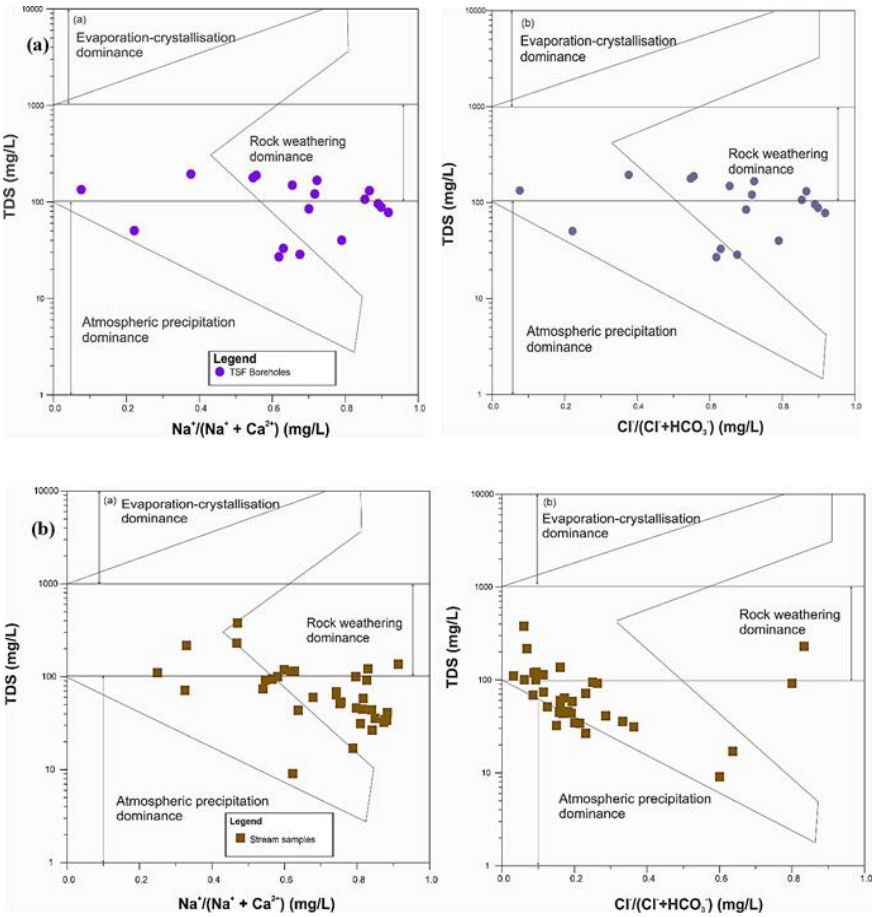

Figure 6: Gibbs Plots for (a) TSF Boreholes and (b) Stream Samples

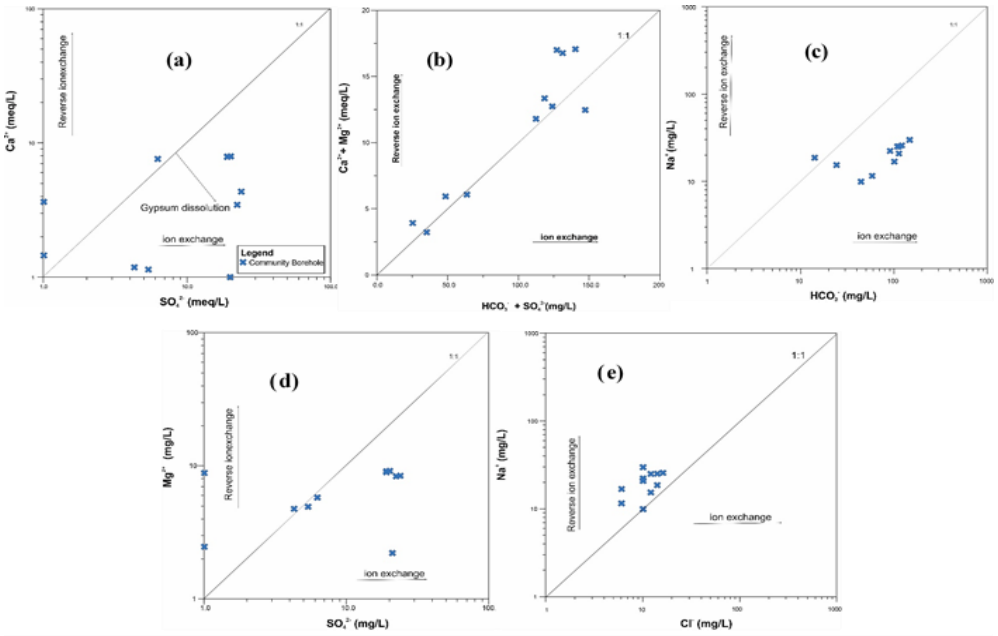

Figure 7: Scatter plots for community Boreholes

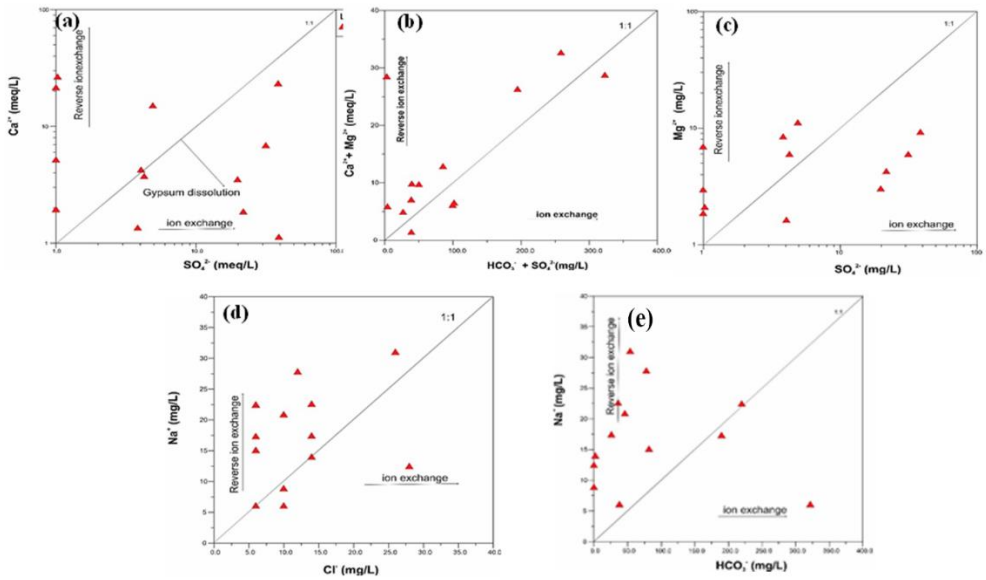

Figure 8: Scatter Plots for Observation Wells

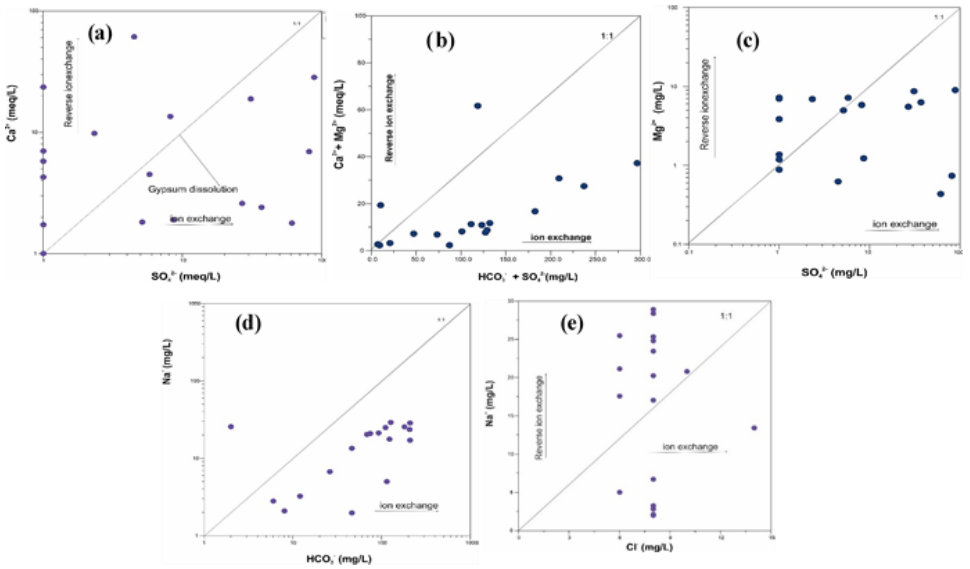

Figure 9: Scatter Plots for TSF

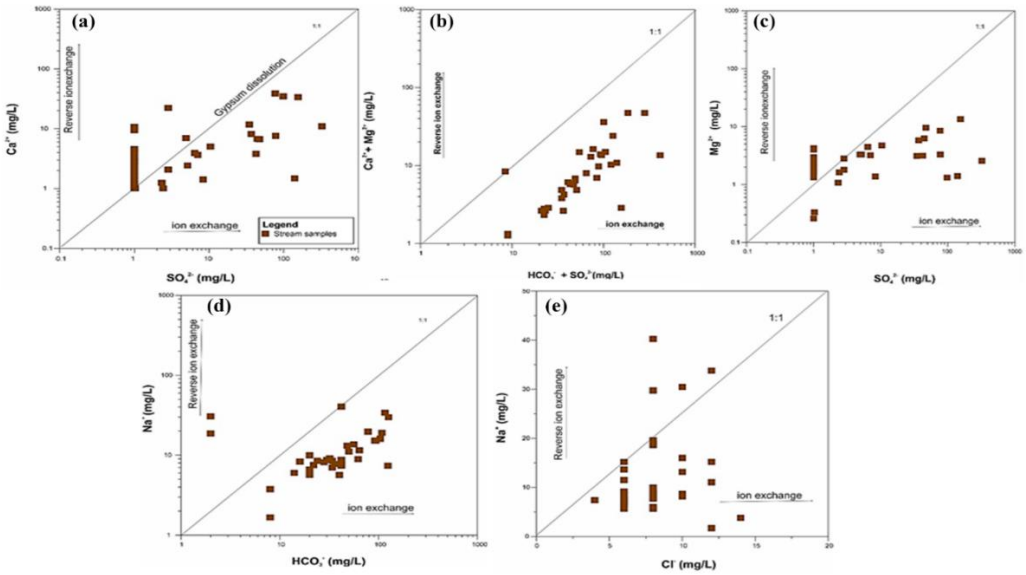

Figure 10: Scatter Plots for Stream Samples

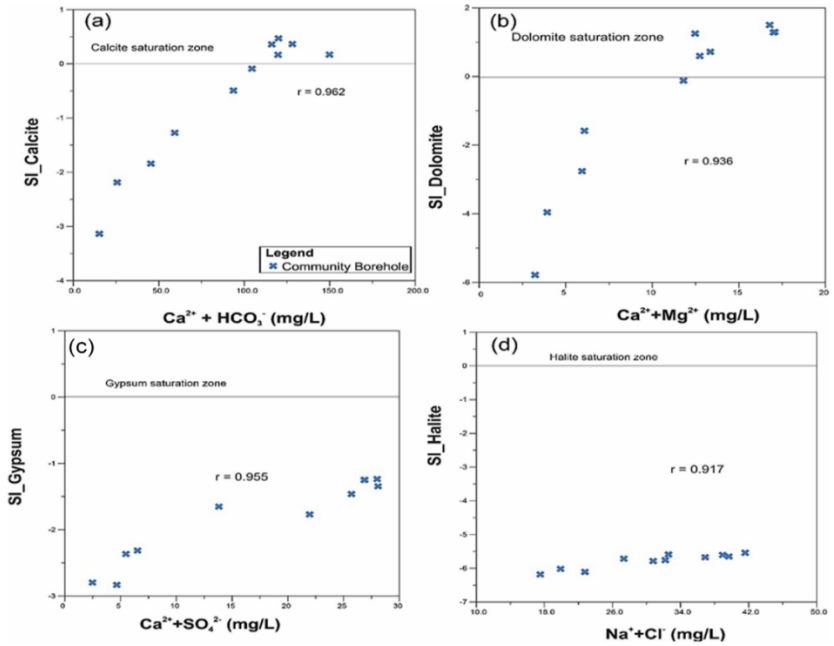

Figure 11: Mineral Saturation for Community Boreholes

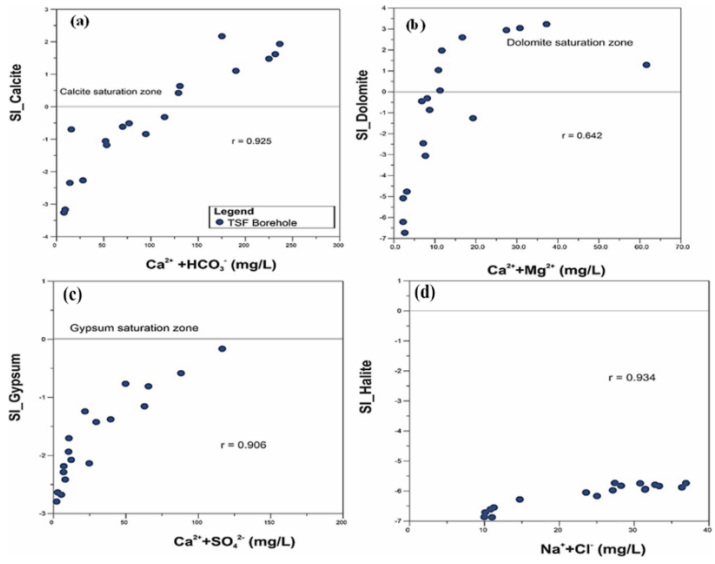

Figure 12: Mineral Saturation for TSF

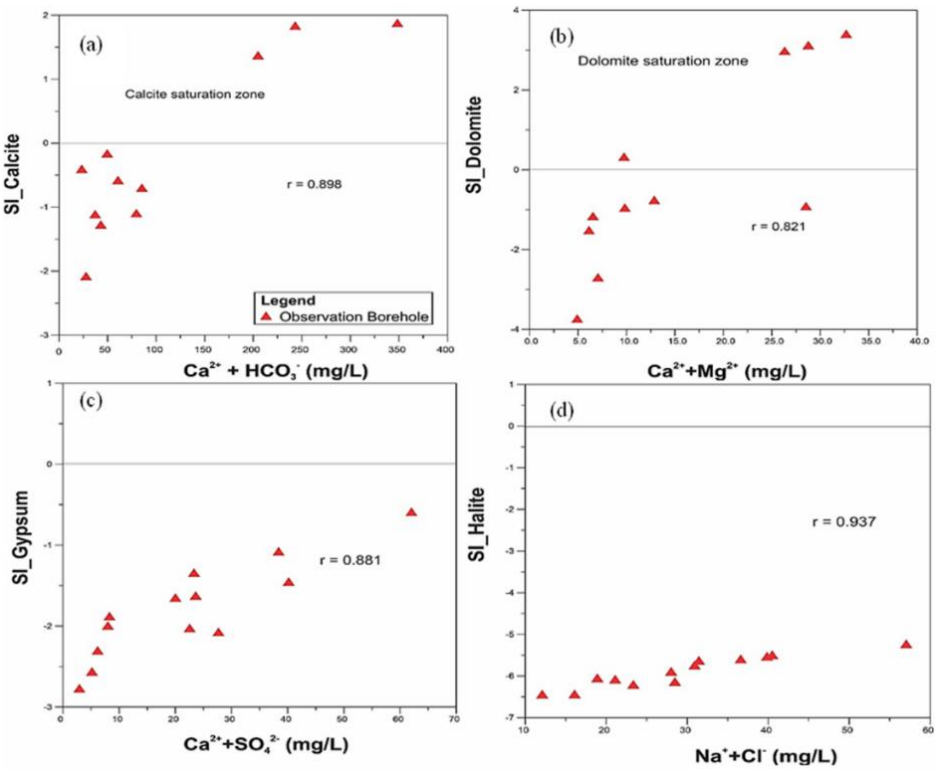

Figure 13: Mineral Saturation for Observation Boreholes

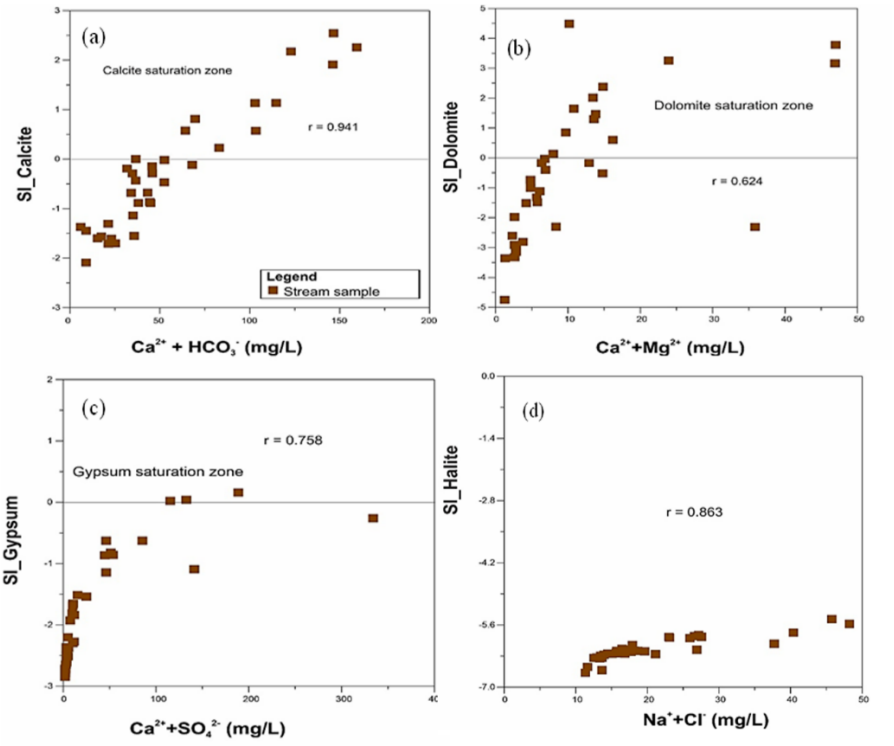

Figure 14: Mineral Saturation for Stream Samples

4.4 Statistical Analyses

4.4.1 Correlation Analysis

A strong positive correlation occurs amongst the following parameters from Table 6: pH and Mg (r = 0.89), pH and HCO3- (0.89), conductivity and TDS (r = 1.00), conductivity and Cl (r= 0.72), TDS and Cl (r = 0.72), K and HCO3- (r = 0.66), K and NO3- (r = 0.84), Mg and HCO3- (r = 0.97), Mg and NO3- (r = 0.73), and HCO3- and NO3- (r = 0.75) except pH and K (r = 0.55). This magnitude of correlation points to similar processes influencing the concentrations of the parameters involved as well as a common source for the parameters involved. i.e., the factors controlling the content of charged ions in the samples are also impacting the amount of TDS present as shown by the correlation between TDS and conductivity and Cl.

4.4.2 Factor Analysis

In all, three (3) components with eigen-values greater than 1 were extracted by the principal component matrix method of factor analysis (Table 7). These factors explain cumulatively 70.866 % of the variance in the hydrogeochemical dataset in this study. While factor 1 accounts for about 36.622 % of the variance in the dataset, factor 2 accounts for 20.774 % of the variance and factor 3 accounts for 13.470 % of the variance (Table 7).

Factor 1 loads strongly with pH, Mg2+, Ca2+, and HCO3- (Figure 15). This factor may indicate geogenic activities probably from the weathering or dissolution of dolomite and calcite which is confirmed by the saturation indices in Figure 13. The affiliation of pH to Mg2+, Ca2+, and HCO3-

suggest that the concentrations of these parameters could result from the inclusion of carbonic acid with the aquifer system. This could be sourced from atmospheric precipitation leaching biologically generated carbonic acid in the soil into the groundwater. Factor 2 is a component of conductivity, TDS, Na, K, and Cl (Figure 15). Factor 2 may be explained as the boundary between geogenic and anthropogenic activities. This also suggest that the Na+, K+, are the source of charged species within the aquifer system. The inclusion of K+ and Cl- could suggest agricultural activities in the area. The presence of Cl- could also indicate the weathering or dissolution of chlorites from metamorphosed rocks in the study area. Factor 3 loads positively with NO3- and SO42- (Figure 15) and indicates the intensity of agricultural activities such as fertilizer usage by the farming residents of Ayanfuri.

Table 6: Pearson Correlation co-efficient

	pH	Cond	TDS	Na	K	Mg	Ca	Cl	SO4	HCO3	NO3
pH	1.00										
Cond	-0.18	1.00									
TDS	-0.19	**1.00**	1.00								
Na	-0.15	-0.12	-0.12	1.00							
K	**0.55**	-0.18	-0.18	0.28	1.00						
Mg	**0.89**	-0.26	-0.26	0.07	0.61	1.00					
Ca	0.28	-0.17	-0.17	0.13	0.08	0.30	1.00				
Cl	-0.19	**0.72**	**0.72**	-0.14	-0.23	-0.32	-0.14	1.00			
SO4	0.23	0.13	0.13	0.13	0.31	0.35	-0.01	-0.11	1.00		
HCO3	**0.89**	-0.31	-0.31	0.06	**0.66**	**0.97**	0.30	-0.35	0.37	1.00	
NO3	0.61	-0.25	-0.25	0.29	**0.84**	**0.73**	0.15	-0.27	0.45	**0.75**	1.00

Table 7: Total variance explained by factor analysis

Component	Initial Eigenvalues			Rotation Sums of Squared Loadings		
	Total	% of Variance	Cumulative %	Total	% of Variance	Cumulative %
1	**4.028**	**36.622**	**36.622**	**3.287**	**29.879**	**29.879**
2	**2.285**	**20.774**	**57.396**	**2.826**	**25.688**	**55.567**
3	**1.482**	**13.470**	**70.866**	**1.683**	**15.299**	**70.866**
4	0.894	8.130	78.996			
5	0.861	7.828	86.824			
6	0.726	6.597	93.422			
7	0.410	3.727	97.149			
8	0.262	2.378	99.526			
9	0.038	0.342	99.868			
10	0.014	0.131	100.000			
11	8.421E-06	7.655E-05	100.000			

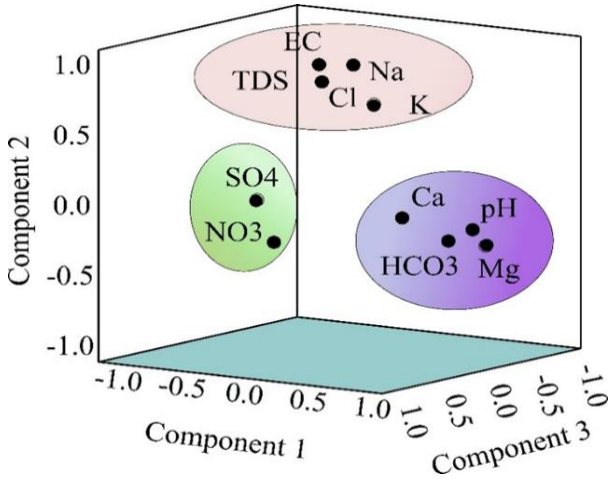

Figure 15: Rotated Component Matrix Plot from Principal Component Analysis

4.4.3 Hierarchical Cluster Analysis

Three (3) clusters were obtained from the hierarchical cluster analysis performed (Figure 16). Cluster 1 loads positively with pH, Mg2+, Ca2+, and HCO3- (Figure 16), bearing strong resemblance to factor 1 from factor analysis (Figure 15). This cluster is an affirmation of the role of geogenic sources such as calcite and dolomite dissolution and ion exchange reactions as enhanced by the acidic nature of the groundwater in the study area. Cluster 2 has conductivity, TDS, Cl-, and SO42- (Figure 16) as it members with some similarity to factor 2 and factor 3 from factor analysis (Figure 15). This cluster could be as a result of gypsum dissolution from the host rock and metamorphosed rocks having chlorite. Cluster 3 accounts for the parameters NO3-, Na+, and K+ (Figure 16) and can be related to factor 2 and 3.

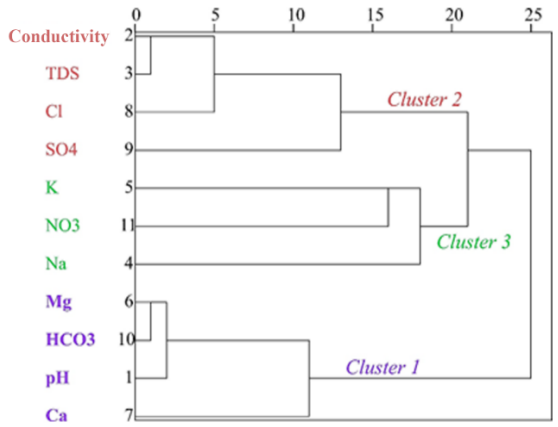

Figure 16: Dendrogram showing three multi-element clusters

4.5 Appraisal of Groundwater Quality for Drinking Purposes

The quality criteria of drinking water have a direct impact on human health. Obtaining safe drinking water is becoming more difficult as a result of human activity. The groundwater samples in this study were examined using both the most desired limit and the highest acceptable limit set for drinking usages by (WHO. 2017). A WQI was also employed to find out the suitability of the groundwater for drinking and other domestic purposes. The quality of drinking groundwater was assessed using the Weighted Arithmetic Index method of the WQI. The WQI is widely used to assess water quality around the world (Keesari et al., 2016). The estimated WQI value of the groundwater samples varies from -47.93 and 27.05 with an average of 3.38 (Table 8). Generally, the calculated WQI values showed that the groundwater in the study area is characterized as excellent quality water since all the estimated values are less than 35 (Brown et al., 1972).

Table 8: Water Quality Index

WQI Range	Type of Water	Samples in this Study
<35	Excellent	77
35-45	Good	0
45-55	Moderate	0
55-65	Poor	0
65-75	Very poor	0
>75	Not Suitable for drinking	0

4.6 Appraisal of Groundwater Quality for Irrigation Purposes

4.6.1 Sodium Adsorption Ratio

The most widely used metric to determine how exchangeable sodium affects the soil's physical state is the sodium adsorption ratio (Richards, 1954). The extra salt in the water reacts with the soil, altering its composition and lowering its permeability. The earth then gets compacted and more impenetrable. Based on the sodium adsorption ratio (SAR), The divided suitable irrigation water into four classes (Table 9) (Richards, 1954). The SAR value of the groundwater sample varies from 0.32 to 7.65 with an average of 2.47 (Table 9). All groundwater samples in the study area fall into the excellent to good category per the categorization since they all had very low SAR values (Table 9) and are of high quality for irrigation purposes in relation to SAR (Richards, 1954).

4.6.2 Magnesium Ratio (MR)

The primary constituents of groundwater are alkaline earth metals. In their native state, Ca2+ and Mg2+ are in balance. These ions are essential for the compaction of soil and plant development. The high Mg2+ content decreases the soil's ability to absorb water when the equilibrium shifts, which ultimately lowers crop output. The presence of exchangeable Na+ in the soil may be the cause of the high Mg2+ concentration in groundwater (Tiwari and Singh, 2014). High magnesium ratio (MR) levels signify soil structural degradation because they are followed by an increase in soil alkalinity. The quality of soil is influenced by the excess quantity of magnesium in water, and the end product is a decrease in crop yields. From the calculated magnesium risk values in the study area, a variation from 1.01 to 86.20 was recorded, with a mean value of 43.98 (Table 9). Based on the classification, a total of 58.44% of the analyzed groundwater samples are appropriate for irrigation purposes (Table 9) (Raghunath, 1987).

4.6.3 Sodium Percentage (Na%)

The large fraction of divalent cations in the groundwater which is Na+ enriched increases the depth of the dispersed double layer on the soil and alters its structure (Simsek and Gunduz 2007; Chacha et al., 2018; Wagh et al., 2018). High Na+ concentrations in the soil solution are notorious for producing soils with weak soil structures. The outcomes are attributed to clays that have prolonged double layers around them expanding to a considerable degree. High sodium percentage (Na%) diminishes the permeability of the soil and alters the internal matrix soil structure, which reduces drainage capacity and finally kills the crops. High EC with high sodium concentration reduces plant growth and alters soil characteristics (Atikul Islam et al., 2017). Na% was proposed by (Wilcox, 1955) as a sodium hazard indicator. The range of the Na% is 8.34% to 91.53%, with an average of 61.12%. (Table 9). This implies that 2.60% of the samples have exceptional quality, 9.09% have good quality, 25.97% have permissible quality, and 54.54% are having doubtful quality with 7.79% being unsuitable. This indicates that about 6 of the samples used in this study are unsuitable for use in crop irrigation.

Table 9: Parameters Influencing Irrigation Suitability

No.	Irrigation Parameter	Classification	Water quality	No. of Samples	Classification
1	Sodium percentage (Na%)	< 20	Excellent	2	Wilcox (1955)
		20–40	Good	7	
		40–60	Permissible	20	
		60–80	Doubtful	42	
		> 80	Unsuitable	6	
2	Sodium adsorption ratio (SAR)	< 10	Excellent	78	Richards (1954)
		11.0–18	Good	0	
		19–26	Doubtful	0	
		> 26	Unsuitable	0	
3	Magnesium Ratio (MR)	< 50	Suitable	45	Szabolcs and Darab (1964)
		> 50	Harmful	32	

5. Conclusions

This research was conducted to identify geochemical processes affecting water quality and the suitability of surface and groundwater for domestic and agricultural use in the Ayanfuri area. The dominant rocks in the area are the underlying schist, phyllites, greywackes, tuffs, and slates and the metavolcanic sequence comprises greenstones of metamorphosed basic lava and intrusive with complementary felsic lava and pyroclastic rocks with minerals of calcite, dolomite, quartz, muscovite, orthoclase, and plagioclase feldspar.

The major cations vary in the order of community boreholes occurring as Na+ > Mg2+ > Ca2+ > K+, and the Observation borehole occurs as Na+ > Ca2+ > Mg2+ > K+, with TSF boreholes occurring as Ca2+ > Na+ > Mg2+ > K+, while streams as Na+ >, Ca2+ >, K+ >, Mg2+. The major anions occur sequentially for all three borehole locations as HCO3- > SO42- > Cl- > NO3- while stream samples occur as SO42- > HCO3- > NO3- > Cl-. The water types in the sampling sites are Na-Mg-HCO3 (54.55%), Na-Mg-HCO3-Cl (23.08%), Na-Mg-HCO3 (22.22%), Na-Mg-HCO3-Cl (22.86%) representing community boreholes, observation boreholes, TSF borehole, and streams, respectively.

The hydrochemical characteristics also show that groundwater formed due to water-rock interaction, atmospheric precipitation patterns, ion exchange processes, and breath dissolution/erosion of plagioclase feldspars. Saturation indices of the mineral phases in the water implied that the water is supersaturated with respect to calcite and dolomite for all borehole samples and the stream samples. Generally, all sampling sites are undersaturated with respect to halite and gypsum except for stream that had about 3 samples been supersaturated. The computed WQI values proved that the groundwater in the study area is categorized as excellent quality water since all the estimated values are less than 35. The water is generally suitable for irrigation; however, SAR suggests the water may be doubtful to unsuitable.

6. Recommendations

Therefore, it is recommended that stakeholders and decision-makers in

the area should aid the people to devise cost-effective technological techniques to treat affected streams and maintain the quality of the other water bodies.

Sources of Funding

This research was funded by the Department of Geological Engineering at the University of Mines and Technology.

Acknowledgement

The authors want to use this opportunity to acknowledge all the efforts of the funding source for making it easy for carrying out this impactful research.

Conflict of Interest

The authors declare no conflict of interest

References

Adu, R.B., 2018. Illegal Gold mining and water quality. A case study of River Offin in the Central Region of Ghana, Doctoral dissertation, Hochschulbibliothek der Technischen Hochschule Köln, Pp.114.

Agyemang, V. O., 2021. Hydrogeophysical characterization of aquifers in Upper Denkyira East and West Districts, Ghana. Applied Water Science, 11(7), Pp.1-14.

Agyemang, V. O., 2022. Application of geostatistical techniques in the assessment of groundwater contamination in the Afigya Kwabre District of Ghana. Applied Water Science, 12(3), Pp.1-12.

Ako, A. A., Shimada, J., Hosono, T., Kagabu, M., Ayuk, A. R., Nkeng, G. E., Eyong, G. E. T., Takounjou, A.L.F., 2012. Spring water quality and usability in the Mount Cameroon area revealed by hydrogeochemistry. Environmental Geochemistry and Health, 34(5), Pp.615-639.

Amponsah, N., Bakobie, N., Cobbina, S. J., and Duwiejuah, A. B., 2015. Assessment of rainwater quality in Ayanfuri, Ghana. American Chemical Science Journal, 6 (3), Pp.172.

Atikul-Islam, M., Zahid, A., Rahman, M.M., Rahman, M.S., Islam, M.J., Akter, Y., Shammi, M., Bodrud-Doza, M. and Roy, B., 2017. Investigation of groundwater quality and its suitability for drinking and agricultural use in the south-central part of the coastal region in Bangladesh. Exposure and health, 9, Pp.27-41.

Balasubramanian, R., and Saravanakumar, V., 2022. Climate Sensitivity of Groundwater Systems in South India: Does It Matter for Agricultural Income?, In Climate Change and Community Resilience. Pp. 143-156. Springer, Singapore.

Barcelona, M. J., John, A.H., Edward, E.G., 1985. Sampling Tubing Effects on Groundwater Samples. Anal. Chem, 57 (2), Pp.460–464.

Brown, R.M., McClelland, N.I., Deininger, R.A. and O'Connor, M. F., 1972. A water quality index—crashing the psychological barrier. In Indicators of environmental quality, Pp. 173-182. Springer, Boston, MA.

Chacha, N., Njau, K.N., Lugomela, G.V. and Muzuka, A.N., 2018. Hydrogeochemical characteristics and spatial distribution of groundwater quality in Arusha well fields, Northern Tanzania. Applied Water Science, 8, Pp.1-23.

Faanu, A., Adukpo, O. K., Tettey-Larbi, L., Lawluvi, H., Kpeglo, D. O., Darko, E. O., and Agyeman, L., 2016. Natural radioactivity levels in soils, rocks and water at a mining concession of Perseus gold mine and surrounding towns in Central Region of Ghana. SpringerPlus, *5*(1), Pp.1-16.

Gibbs, R. J. (1970). Mechanisms controlling world water chemistry. Science 17. pp.1088-1090.

Hagan, G. B., Minkah, R., Yiran, G. A., and Dankyi, E., 2022. Assessing groundwater quality in peri-urban Accra, Ghana: Implications for drinking and irrigation purposes. Groundwater for Sustainable Development, 100761.

Harter, T.,2003. Groundwater quality and groundwater pollution. https://doi.org/10.3733/ucanr.8084

Jankowski, J., Acworth, R. I. and Shekarforoush, S., 1998. Reverse ion-exchange in deeply weathered porphyritic dacite fractured aquifer system, Yass, New South Wales, Australia. In: Arehart GB, Hulston JR (eds) Proceedings of 9th international symposium on water–rock interaction. Taupo, New Zealand, 30 March–April1998. Balkema, Rotterdam, Pp 243–246.

Keesari, T., Ramakumar, K. L., Chidambaram, S., Pethperumal, S., Thilagavathi, R., 2016. Understanding the hydrochemical behavior of groundwater and its suitability for drinking and agricultural purposes in Pondicherry area, South India–A step towards sustainable development. Groundwater Sustain. Dev. 2, Pp.143–153.

Kumar, P. S., and Balamurugan, P., 2018. Evaluation of groundwater quality for irrigation purpose in attur taluk, Salem, Tamilnadu, India. Water and Energy International, 61(4), Pp. 59-64.

Kumar, R. S., Sudheer, C. V., Ramana, G. V., and Ramya, N., 2022. Comparative Study of Physical and Chemical Parameters of Lakes in Medchal District. In Advanced Modelling and Innovations in Water Resources Engineering, Pp. 635-643. Springer, Singapore.

Laskar, N., Singh, U., Kumar, R., and Meena, S. K., 2022. Spring water quality and assessment of associated health risks around the urban Tuirial landfill site in Aizawl, Mizoram, India. Groundwater for Sustainable Development, 100726.

Li, P., Wang, D., Li, W. and Liu, L., 2022. Sustainable water resources development and management in large river basins: an introduction. Environmental Earth Sciences, 81(6), Pp.1-11.

Li, P., Wu, J. and Qian, H., 2016. Hydrochemical appraisal of groundwater quality for drinking and irrigation purposes and the major influencing factors: a case study in and around Hua County China. Arab. J. Geosci. 9 (1), Pp.15.

Liu, J., Gao, Z., Wang, Z., Xu, X., Su, Q., Wang, S. and Xing, T., 2020. Hydrogeochemical processes and suitability assessment of groundwater in the Jiaodong Peninsula, China. Environmental monitoring and assessment, 192(6), Pp.1-17.

Okofo, L. B., Bedu-Addo, K., and Martienssen, M., 2022. Characterization of groundwater in the 'Tamnean' Plutonic Suite aquifers using hydrogeochemical and multivariate statistical evidence: a study in the Garu-Tempane District, Upper East Region of Ghana. Applied Water Science, 12(2), Pp. 1-22.

Parkhurst, D. L. and Appelo, C. A. J., 1999. User's Guide to PHREEQC (Version 2): A Computer Program for Speciation, Batch-Reaction, One-Dimensional Transport, and Inverse Geochemical Calculations. Water-Resources Investigations Report. US Geological Survey, Denver, Pp.99–4259.

Piper, A. M., 1944. A graphic procedure in the geochemical interpretation of water analysis (No. 12). US Department of the Interior, Geological Survey, Water Resources Division, Ground Water Branch.

Raghunath, H. M., 1987. Groundwater. Wiley Eastern Ltd., Delhi, Pp.563

Rahaman, M. H., Sajjad, H., Masroor, M., Bhuyan, N. and Rehman, S., 2022. Delineating groundwater potential zones using geospatial techniques and fuzzy analytical hierarchy process (FAHP) ensemble in the data-scarce region: evidence from the lower Thoubal river watershed of Manipur, India. Arabian Journal of Geosciences, 15(8), Pp.1-20.

Rathnasri, P. A. S. A. and Manage, P. M., 2016. Evaluation of groundwater quality in five grama divisions of Maharagama urban area using groundwater quality index (WQI).

Richards, L. A. 1954. Diagnosis and improvement of saline and alkali soils. Washington D.C.

Simsek, C. and Gunduz, O., 2007. IWQ index: a GIS-integrated technique to assess irrigation water quality. Environmental monitoring and assessment, 128, Pp.277-300.

Sunkari, E. D., Seidu, J., and Ewusi, A., 2022. Hydrogeochemical evolution and assessment of groundwater quality in the Togo and

Dahomeyan aquifers, Greater Accra Region, Ghana. Environmental Research, 112679.

Szabolcs, I., and Darab, K., 1964. Radio-Active technique for examining the improving effect of CaCO3 on alkali (Szik) soils. Acta Agron. Hung, 13, Pp.93-101.

Tiwari, A. K. and Singh, A. K., 2014. Hydrogeochemical investigation and groundwater quality assessment of Pratapgarh district, Uttar Pradesh. J Geol Soc India, 83(3), Pp.329-343.

Wagh, V. M., Panaskar, D. B., Mukate, S. V., Gaikwad, S. K., Muley, A. A. and Varade, A. M., 2018. Health risk assessment of heavy metal contamination in groundwater of Kadava River Basin, Nashik, India. Modeling Earth Systems and Environment, 4, Pp. 969-980.

WHO (World Health Organization). 2017. Guidelines for drinking water quality. Incorporating the first addendum, 4th edn. WHO, Geneva.

Wilcox, L. V., 1955. Classification and use of irrigation water. US Geol. Dept. Agric. Circ. 969, Pp. 19.